Journal of Information Technology Management

Print ISSN: 2008-5893

Online ISSN: 2423-5059

Efficient NetB3 for Enhanced Lung Cancer Detection: Histopathological Image Study with Augmentation

Bhavani Rupa Devi

Department of CSE Annamacharya Institute of Technology and Sciences, Tirupati, India. E-mail: rupadevi.aitt@annamacharyagroup.org

Karthik Sagar Ashok

Department of Information Science and Engineering, BMS Institute of Technology and Management, Bengaluru, Karnataka. E-mail: karthiksa@bmsit.in

Seemanthini Krishne Gowda

Department of Machine Learning (AI-ML) BMS College of Engineering, Bangalore, India. E-mail: seemanthinik.mel@bmsce.ac.in

Konatham Sumalatha

Department of Database Systems, School of Computer Science and Engineering, Vellore Institute of Technology, Vellore - 632014, Tamilnadu, India. E-mail: konatham.sumalatha@vit.ac.in

Ganesan Kadiravan

Department of Computer Science and Engineering, Koneru Lakshmaiah Education Foundation, Vaddeswaram, AP, India. E-mail: kadiravanphd@gmail.com

Ranjith Kumar Painam*

*Corresponding author, Department of Electronics and Communication Engineering, Kallam Haranadhareddy Institute of Technology (Autonomous), NH-16, Chowdavaram, Guntur, Andhra Pradesh, India. E-mail: ranjithkumar.painam@gmail.com

Abstract

Cancer is an abnormal cell growth that occurs uncontrollably within the human body and has the potential to spread to other organs. One of the primary causes of mortality and morbidity for people is cancer, particularly lung cancer. Lung cancer is one of the non-communicable diseases (NCDs), causing 71% of all deaths globally, and is the second most common cancer diagnosed worldwide. The effectiveness of treatment and the survival rate of cancer patients

can be significantly increased by early and exact cancer detection. An important factor in specifying the type of cancer is the histopathological diagnosis. In this study, we present a Simple Convolutional Neural Network (CNN) and EfficientNetB3 architecture that is both straightforward and efficient for accurately classifying lung cancer from medical images. EfficientnetB3 emerged as the best-performing classifier, acquiring a trustworthy level of precision, recall, and F1 score, with a remarkable accuracy of 100%, and superior performance demonstrates EfficientnetB3's better capacity for an accurate lung cancer detection system. Nonetheless, the accuracy ratings of 85% obtained by Simple CNN also demonstrated useful categorization. CNN models had significantly lower accuracy scores than the EfficientnetB3 model, but these determinations indicate how acceptable the classifiers are for lung cancer detection. The novelty of our research is that less work is done on histopathological images. However, the accuracy of the previous work is not very high. In this research, our model outperformed the previous result. The results are advantageous for developing systems that effectively detect lung cancer and provide crucial information about the classifier's efficiency.

Keywords: Lung Cancer, Convolutional Neural Network (CNN), Histopathological Images, Transfer Learning, Lung Cancer Detection

Journal of Information Technology Management, 2024, Vol. 16, Issue 1, pp. 98-117
Published by University of Tehran, Faculty of Management
doi: https://doi.org/ 10.22059/jitm.2024.96377
Article Type: Research Paper

Received: December 17, 2023
Received in revised form: January 06, 2024
Accepted: February 02, 2024
Published online: February 29, 2024

Introduction

The primary organs of respiration are the lungs. In the human body, one lung is situated on each side of the chest. The lungs are responsible for oxygenating the blood. The heart pumps blood to the lungs, which contain a significant amount of carbon dioxide and little oxygen (Dimililer, 2017). Some of the most common malignancies are lung, breast, stomach, and prostate cancers, which, if not caught early, can cause serious complications or, in many cases, death. In the human body, cancer is a manifestation of aberrant cell proliferation (Singh, 2019). Nearly 25% of all cancer-related deaths occur from lung cancer, making it a common malignancy in both men and women. The leading cause of death from malignant tumors in males is lung cancer and breast cancer in females. Lung cancer can be quite harmful, and one of the main reasons for this is that it is latent, and its early-stage signs are difficult to recognize. Most individuals progress to the intermediate and severe stages when clear-cut clinical symptoms appear. At this point, the prognostic impact is also very poor, the effect of therapy is very limited, and the cure rate is severely reduced. As a result, patients'

response to treatment can be greatly enhanced by detecting and diagnosing lung cancer at an early stage (Rong, 2021).

There are over 1.8 million new cases of lung cancer each year, which causes 1.6 million fatalities globally. Abnormal growth and development of cells in tumors is the reason for lung cancer and the highest mortality rate among all cancers. With a mortality rate of 19.4%, lung cancer is among the most terrible diseases in poor nations. With the lowest success rate after diagnosis and an annual increase in casualties, lung cancer is the deadliest cancer globally (Kalaivani, 2020). Additionally, Nearly 80% of lung cancer deaths were caused by smoking. Nonsmokers are at increased risk of lung cancer due to other factors such as radon, secondhand smoke, air pollution or exposure to asbestos at work, exposure to diesel exhaust, or exposure to certain chemicals (Viale, 2020).

Non-small cell lung cancer (NSCLC) and small cell lung cancer (SCLC) are the two principal types of lung cancer. The growth and spread of each type of lung cancer varies, as does how it is handled. Assorted small cell/large cell cancer refers to cancer with traits from both types. Comparatively more prevalent and often growing and dispersing more slowly than SCLC is non-small cell lung cancer. The expansion rate of SCLC and the shape of large tumors, which can disseminate widely throughout the body, are directly associated with cigarette smoking. In the bronchi towards the chest's center, they frequently begin. Lung cancer mortality is completely influenced by cigarette smoking (Krishnaiah, 2013).

When a patient has a chest X-ray or CT scan for any other valid cause, lung cancer is frequently detected. When the remaining 75% of people exhibit or acquire symptoms, they are diagnosed. As cutting-edge algorithms and Artificial Intelligence (AI) systems are combined to empower clinicians, a transformative wave is expected to reshape the healthcare landscape over the decade. These technologies include Higher-Order Statistics (HOS) (de la Rosa, 2013), Fuzzy logic (FL) (Bhaktavastalam, 2016), Artificial Neural Networks (ANN) (Prisciandaro, 2023), Genetic Algorithms (GA), and Computer-Aided Diagnosis (CAD) among others (AlZubaidi, 2017). Their harmonious collaboration should improve patient care by increasing the accuracy of diagnoses and the effectiveness of treatments. Machine Learning (ML) and Deep Learning (DL), an extraordinary subset of AI, are at the core of this symphony and orchestrate machines to glean insights without explicit programming, a metamorphosis achieved through immersion in varied datasets and skill-honed through experiential learning (Roy, 2021). Most of the authors' earlier work used machine learning techniques with x-ray and CT scan images. Support Vector Machine (SVM) (Manju, 2021), Random Forest (RF) (Bhattacharjee, 2022), Bayesian Networks (BN), and Convolutional Neural Networks (CNN) (Shandilya, 2022) combine in this instance to create a ballet of illuminating approaches that reveal the secrets hidden in these photos and unleash their potential for lung cancer diagnosis and categorization.

Research Objectives and Motivation

Two primary objectives drive this research:

To significantly enhance lung cancer detection accuracy by implementing advanced DL techniques, specifically CNN and the state-of-the-art EfficientNetB3 architecture.

Evaluating the consequence of innovative data augmentation techniques on improving the performance of DL models for the detection of lung cancer is a critical step toward improving patient outcomes.

The motivation behind this study lies in the compelling need to address the global health burden caused by lung cancer. Early detection of lung cancer can guide to more satisfactory treatment and ultimately reduce survival.

Contribution

This study presents several significant contributions to lung cancer detection. It uses advanced DL techniques, including state-of-the-art architectures such as EfficientNetB3 and CNN, to accurately classify lung cancer based on histopathological images. Through a comparative analysis, we establish the suitability of these models for accurate lung cancer detection. Additionally, our research introduces innovative data augmentation methods to enhance model performance by expanding the dataset through augmentation, and this aims to improve the models' ability to predict previously unseen data. Our experimental results showcase the exceptional accuracy of the EfficientNetB3 model, achieving a remarkable 100% accuracy rate in lung cancer detection. This outstanding outcome underscores the potential for highly reliable diagnostic systems for lung cancer. Lastly, the clinical relevance of our findings is substantial, as they hold promise for the development of AI-powered tools that can aid healthcare professionals in early and precise lung cancer diagnosis.

To structure this paper, we have separated it into multiple sections. Firstly, in Section 2, we will review the different approaches to detecting lung cancer. Observing this, we will summarize our methodology statement in Section 3. Section 4 will explain the experimental outcomes of our utilized models and compare our outcomes with existing work. Finally, we will conclude by proposing our findings.

Literature Review

To enhance the accuracy of lung cancer detection within CT scan images, the study (Makaju, 2018) examined the use of computer-aided diagnosis (CAD) approaches, noting the difficulties doctors experience in making an accurate diagnosis. A unique model is put forth after a review of current CAD approaches, including watershed segmentation for nodule

detection and SVM for determining whether a nodule is cancerous or benign. With a superior 92% detection accuracy compared to the current model and an 86.6% classification accuracy, it represented a significant step forward in improving the accuracy and reliability of lung cancer diagnosis. It also holds the potential to have a significant impact on medical imaging and diagnostics. Another study (Ahmed, 2022) presented the Genetic K-Nearest Neighbor (GKNN) Algorithm, which can identify early-stage lung cancer in CT lung images. The suggested model effectively and quickly categorizes cancer images by integrating the Genetic Algorithm with the K-Nearest Neighbor (K-NN) approach. The solution employed the image processing toolkit in MATLAB on CT lung pictures, focusing on performance measures like classification and false positive rates. This method, which chose K-nearest samples (50–100) using a Genetic Algorithm, allowed the model to attain a noteworthy 90% classification accuracy.

The study (Kumar, 2023) proposed a novel automated diagnostic method for lung CT images to address the urgent need for early lung cancer identification. This technique takes advantage of deep features recovered from CT lung images and uses LDA to minimize feature dimensionality by integrating Optimal Deep Neural Network (ODNN) and Linear Discriminant Analysis (LDA). The Modified Gravitational Search Algorithm (MGSA) is used to optimize the ODNN for lung cancer categorization further. Results showed a convincing sensitivity of 96.2%, a specificity of 94.2%, and an outstanding accuracy of 94.56%. This cutting-edge combination of methods highlighted a promising trend in lung cancer diagnosis and offers patients a better chance of surviving the disease.

According to (Bhuvaneswari, 2015), the dataset from the Lung Image Database Consortium (LIDC) is used to analyze the usefulness of DL algorithms in detecting lung cancer. CNN, deep belief networks (DBNs), and stacked denoising autoencoders (SDAE) are three DL models that were applied and corresponded to a conventional computer-aided diagnosis (CADx) system using 28 image features and SVM. The acquired accuracies for CNN, DBNs, and SDAE were 0.7976, 0.8119, and 0.7929, whereas the accuracy of the conventional CADx was 0.7940, only somewhat lower than that of CNN and DBNs.

The study (Lakshmanaprabu, 2019) concentrated on using ML approaches to build efficient models for early detection of high-risk patients susceptible to lung cancer, permitting prompt actions to attenuate long-term effects and described the Rotation Forest approach and assessed the effectiveness of the strategy using well-known measures. The evaluation demonstrated the proposed model's amazing efficacy with an impressive AUC of 99.3%.

Another investigation by (Sun, 2016) used the Kaggle Data Science Bowl 2017 dataset with unlabeled nodules and demonstrated a computer-aided diagnosis (CAD) method designed for lung cancer categorization in CT scans. Lung tissue is distinguished from the rest of the image using thresholding as an initial segmentation technique. To find potential

nodules within the segmented scans, the study used a modified U-Net trained on LUNA16 labeled data. 3D Convolutional Neural Networks (CNNs) are then applied to the possible nodule locations that the U-Net discovered to classify lung cancer. The 3D CNNs manage an impressive accuracy of 86.6% on the test set despite issues like false positives.

In Table 1, we discussed the dataset, data augmentation, and segmentation techniques of existing research work.

Several significant limitations come with the present investigation that are worth acknowledging. The study cannot forecast the nature, arrangement, or dimensions of tumors, which is a critical factor in the early diagnosis and treatment of cancer. Additionally, the research was limited by a restricted number of pixels in its analytical approach, which may not be conducive to early cancer detection. The lack of appropriately labeled datasets, especially for lung cancer images, presents a significant

Table 1. Overview of Existing work: Dataset, Augmentation and Segmentation Techniques

Dataset	Augmentation	Segmentation
WSI dataset	OTSU's method	Rotation, translation, flipping and color jittering
LIDC dataset	Rotation, shear, zoom range , and horizontal and vertical flip	Data Science Bowl Kaggle competition's method
The National Lung Cancer Screening Trial (NLST) and Early Lung Cancer Action Program (ELCAP)	Rotation	Location and size
LUNA16 dataset and the LIDC-IDRI	Random cropping of zero-padded nodules	Various radio densities of different substances
LC25000 Lung and colon histopathological image dataset	Flip in horizontal and vertical and a zoom range	Area, perimeter, and eccentricity
LIDC-IDRI datasets	Translation, rotation, flipping, and cropping	Various radio densities of different substances

Obstacle when training machine learning models. Obtaining accurately annotated training data is also challenging due to the resource-intensive nature of annotating genomic data, which is closely linked with histological images. Access-related challenges when dealing with extensive databases also hinder the effectiveness of classification algorithms for histological images across various healthcare settings. Integrating machine learning platforms with high-performance computing in extensive healthcare facilities has promising benefits. The primary focus should be devising innovative solutions to overcome these challenges, ultimately improving the precision and efficiency of diagnostic procedures.

Methodology

In this part, we discuss our suggested methods for detecting lung cancer using cutting-edge DL models. Our method seeks to transform the early identification and treatment of lung cancer by utilizing the synergy of advanced image analysis and artificial intelligence. Using a well-organized pipeline, we describe the procedures for converting unprocessed medical image data into useful diagnostic data. The overall steps performed in our research are shown graphically in Figure 1. We will describe each step of the research below:

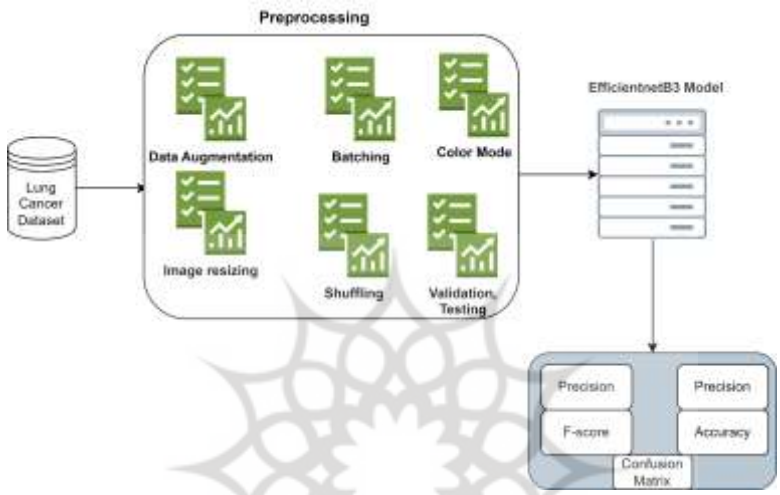

Figure 1. Overall steps of our research

Dataset and Data Preprocessing

Dataset Description:

To diagnose and comprehend a variety of medical diseases, histopathological investigation is crucial. We used the Lung and Colon Cancer Histopathological Image Dataset (LC25000) for our work, and this dataset has 25,000 jpeg files that are 768 x 768 pixels in size and contain five different types of histopathology images (Borkowski, Lung and colon cancer histopathological image dataset, 2019). A wide range of histopathological images is added to this dataset, which was created from sources that were extensively validated and HIPAA-compliant, containing 750 total images of lung tissue, including 250 benign lung tissue, 250 lung adenocarcinomas, and 250 lung squamous cell carcinomas.

There are also 500 colon tissue images, including - 250 benign colon tissue and 250 colon adenocarcinomas.

The dataset was supplemented with the Augmentor package to 25,000 images to increase its size and improve its diversity and usability. The dataset consists of five classes with 5,000 images each, including Lung benign tissue, Lung adenocarcinoma, Lung squamous cell carcinoma, Colon adenocarcinoma, and colon benign tissue.

Some dataset samples are shown in Figure 2.

Dataset Preprocessing:

This code snippet's preparation pipeline for image data includes numerous crucial steps that prepare the images for a machine learning model's training and evaluation. The target image size is initially set to 224x224 pixels with three color channels (RGB), with batch size 16. Training, validation, and test sets of data have been created. An Image Data Generator is used for each set to apply different preprocessing methods.

The real-time data augmentation enhances the resilience and generalization of the model that the Image Data Generator does during training. Each image batch is subjected to arbitrary rotations, shifts, flips, and zooms as part of data augmentation. This lessens overfitting by exposing the model to a larger range of variability in the data. Data augmentation is turned off during testing to guarantee that the model's forecasts are accurate and comparable.

Data stored in dataframes (train df, valid df, and test df) are utilized to generate batches of images and the labels that go with them using the flow from dataframe function. The file paths supplied in the dataframe columns are used to load the images, and the 'categorical' class mode is used to one-hot encode the labels. Important aspects of the preprocessing methods:

1. Image resizing: To provide uniform input dimensions for the Model, images are scaled to a consistent size of 224x224 pixels.
2. Color Mode: Each image's red, green, and blue channels are preserved while reading an image in RGB color mode.
3. Data Augmentation: To improve model resilience, data augmentation is used during training (train gen), adding variations in rotations, shifts, flips, and zooms.

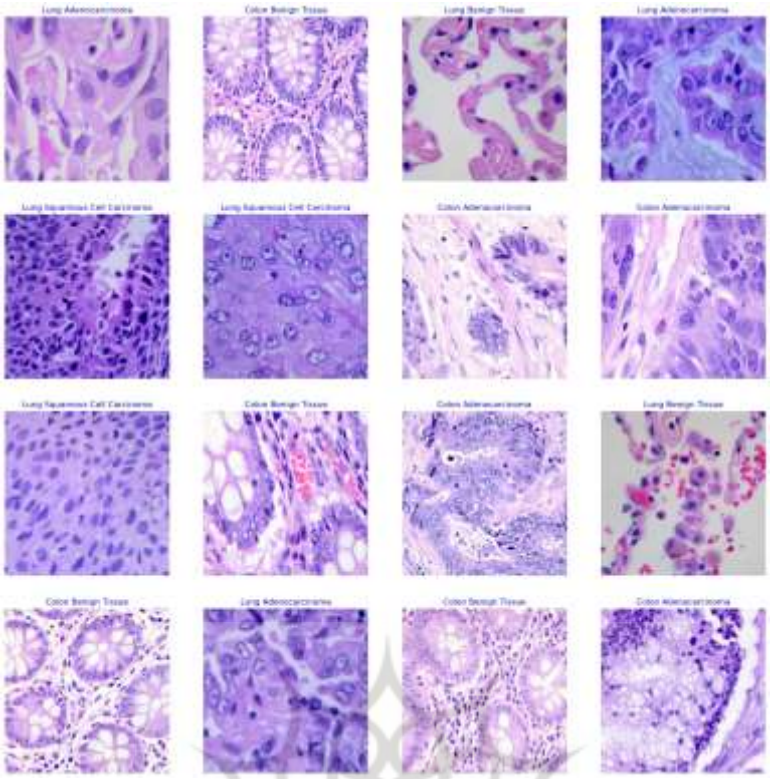

Figure 2. Samples of the dataset

4. Batching: During training, validation, and testing, 16 images are loaded in batches. During training, batch processing provides effective GPU use and gradient updates.
5. Shuffling: To prevent the model from memorizing the order of the images and increase generalization, images are randomly shuffled inside each batch.
6. Validation and Testing: Shuffling is deactivated to accurately assess the model's performance for validation (valid gen) and testing (test gen), and images are processed without data augmentation.

Proposed Model SimpleCNN Model

In this study, we provide a CNN architecture that is both straightforward and efficient for accurately classifying lung cancer from medical images. Layer by layer, we describe the model's construction and offer the relevant mathematical equations that describe how it works. The architecture demonstrates the effectiveness of fundamental CNN building blocks in producing accurate and reliable categorization outcomes. Our study uses DL to tackle the crucial task of classifying lung cancer. The suggested architecture takes advantage of CNNs' innate ability to recognize complex patterns in medical pictures, providing a framework for cutting-edge diagnosis. The structure of the architecture is as follows:

1. Convolutional Layers: Convolutional layers are first used in the model to extract hierarchical characteristics from the input photos. Every 2D convolutional operation is

followed by an activation and normalization process in each convolutional layer. The first convolutional layer uses a collection of 32 filters to produce a 3x3 convolution on the input image tensor X. Non-linearity is introduced by the ReLU activation function (A), and the training process is stabilized with the help of batch normalization (BN). The following is the equation for this operation:

$$C_1 = \mathrm{A}\,(\mathrm{BN}(\mathrm{Conv2D}(X, 32, (3,3)))) \quad (1)$$

The input image tensor is represented by the variable X. The raw picture data we feed into a convolutional neural network (CNN) for processing is referred to as X in this context. On this input image, the Conv2D layer performs a 2D convolution operation. The output of the convolutional operation is then subjected to the BN and ReLU (rectified linear activation) functions. Although the number of filters in the following convolutional layers (C2 and C3) is higher (64 and 128, respectively), they follow a similar pattern. After each convolutional block, the MaxPooling operation (MP) with a 2x2 pooling window is used to downsample the spatial dimensions of the feature maps. The following is the equation for this operation:

$$\mathrm{MP}(\mathrm{A}(\mathrm{BN}(\mathrm{Conv2D}(C_1, 64, (3,3))))) \quad (2)$$
$$\mathrm{MP}(\mathrm{A}(\mathrm{BN}(\mathrm{Conv2D}(C_2, 128, (3,3))))) \quad (3)$$

2. MaxPooling Layers: MaxPooling is carried out by moving a window of a predetermined size across the feature map (often 22 or 33). The highest value in the window is chosen at each stage, which is subsequently kept in the final downscaled feature map. This approach reduces the feature map's dimensionality while keeping the most crucial details. This procedure is represented mathematically as follows:

$$P_i = \mathrm{MaxPool2D}\,(C_i, \text{pooling window} = (2,2)) \quad (4)$$

It shows how the feature map Ci was subjected to the MaxPooling technique. Ci, in this case, represents the output of the preceding convolutional layer (C1 or C2), and the pooling window is set to (2, 2), suggesting that a window of size (2 times 2) is utilized to extract features from the downsampled image. The final product, Pi, is a downscaled version of the feature map Ci that keeps the highest value from each pooling window. The feature map's spatial dimensions are effectively reduced due to this procedure, which encourages effective computing and improves the network's capacity to recognize key patterns while ignoring less crucial information.

3. Flatten and Dense Layers: The feature maps are converted into a one-dimensional (1D) vector after extracting pertinent features using convolutional and pooling layers to permit further processing by dense (completely connected) layers. This transformation is essential since it enables the model to use these features for classification tasks. The flattening process is modelled mathematically as follows:

$$F = \text{Flatten}(P^n) \quad (5)$$

The first dense layer (D1), which serves as a feature fusion step and receives the flattened feature vector F afterward. Through the ReLU (Rectified Linear Unit) activation function, this dense layer adds nonlinearity to the features. The ReLU activation function improves the model's capacity to extract pertinent data and aids in the collection of complex patterns within the data. This operation can be described mathematically as:

$$D_1 = \text{ReLU}(\text{Dense}(F, 128)) \quad (6)$$

Where D1 denotes the first dense layer's output, and 128 denotes the layer's total number of neurons (or units). After passing through the second dense layer (D1), the output of D2, which contains fused and non-linearly modified features, is produced. By further honing the features, this layer enables the model to recognize higher-level patterns that are essential for precise classification. The ReLU activation function introduces non-linearity similar to the prior layer. This operation is represented mathematically as follows:

$$D_2 = \text{ReLU}(\text{Dense}(D_1, 64)) \quad (7)$$

Here, D2 results from the dense layers, and 64 is the number of neurons in this second dense layer.

4. Output Layer: The model's computations are completed in the output layer, which generates class probabilities that allow the model to make predictions about the input data. The outputs of the model's last layer are converted into class probabilities in a crucial way by the softmax activation function. The softmax function normalizes a vector of scores or logits to reflect probabilities that add up to 1. Each component of the output vector represents the likelihood that the input belongs to a particular class. Here is the softmax equation:

[redacted] (8)

N is the total class number, and zi is the score (logit) corresponding to class i.

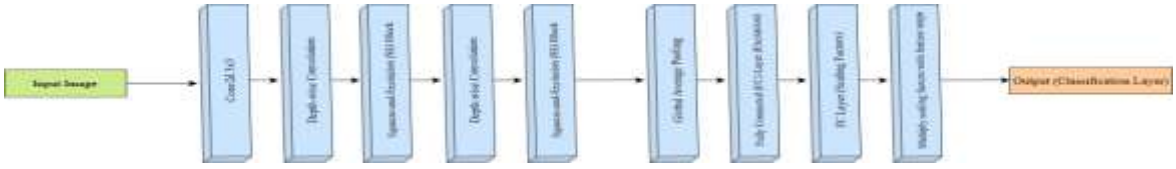

Figure 3. Proposed model efficientnetB3 architecture

Efficient netB3

We outline the design of our suggested lung cancer detection model in this section. The model is made to accurately classify medical images by quickly extracting and learning key elements from the images. Because it has been demonstrated to balance model size and performance in computer vision applications successfully, we use the EfficientNetB3 architecture as the foundation.

Convolutional neural network (CNN) architecture EfficientNetB3 is a member of the EfficientNet family. It was created to strike a fair compromise between model size and effectiveness for various computer vision tasks, including object identification and image categorization. Compared to less advanced models like EfficientNetB0 and EfficientNetB1, EfficientNetB3 is more sophisticated and potent. Like other EfficientNet models, EfficientNetB3's architecture is distinguished by three essential elements: Depth-wise Convolution, SE blocks, and compound scaling of width, depth, and resolution. Let's dissect these elements and comprehend those using visuals as well as textual descriptions:

1. Depth-wise Convolution: The fundamental units of the model's convolutional layers are depth-wise separable convolutions. This method requires two sequential steps: point-wise convolution, which combines the output channels, and depth-wise convolution, which applies a convolutional filter to each input channel independently. As a result, the computational cost is significantly decreased while the expressive capability of the network is maintained.
2. Squeeze-and-Excitation (SE) Blocks: Squeeze-and-Excitation (SE) blocks are used in the model to improve feature representation in the network. The SE blocks are divided into two stages: the squeeze stage uses global average pooling to produce statistics for each channel, and the excitation stage uses fully connected layers to mimic channel dependencies. The feature maps' relevance is clarified using the derived scale factors.
3. Compound Scaling: By modifying the breadth, depth, and resolution coefficients, we use compound scaling to further adapt the model to our job. The careful selection of these coefficients, designated as phi, psi, and rho, respectively, ensures optimal performance and computing efficiency. The following equation is used to determine the output resolution:

$$Resolution = 300 \times (1.15^{\phi}) \quad (9)$$

The EfficientNetB3 model, a cutting-edge neural network that has undergone pre-training on the expansive ImageNet dataset, forms the basis of the model design. The network can automatically learn and recognize complicated patterns from images using feature extraction, which is made possible by the pre-trained model that acts as its foundation. The original fully connected layers of EfficientNetB3 are removed by setting 'include top' to 'False,' transforming the model into a specialized feature extractor. A Batch Normalization layer is

added after the underlying model. By minimizing the internal covariate shift, batch normalization improves training stability and speed. It works by normalizing the output of the preceding layer. The next step is to create a highly connected layer with 256 neurons. L2 weight regularization, L1 activity regularization, and L1 bias regularization are three more regularization types that are enhanced in this layer. These regularization terms can be represented mathematically as follows.

(a) L2 weight regularization:Loss += $0.016 \cdot \| \text{weights} \|^2$

(b) L1 activity regularization: Loss += $0.006 * \cdot activities \cdot (L1norm)$

(c) L1 bias regularization: Loss += $0.006 * \cdot biases \cdot (L1norm)$

To prevent large weight magnitudes, promote sparse activations, and discourage biased activations all of which contribute to overfitting—these parameters are added to the loss function. Rectified Linear Activation (ReLU) is the activation function that was used in this instance. Subsequently, a Dropout layer is included, which aids in preventing overfitting by randomly deactivating a fraction of input units during each training iteration. This addition of stochasticity encourages the network to learn more reliable features.

Another densely coupled layer acts as the output layer, with a neuron count equal to the total number of classes, making up the final layer. This layer makes a prediction about the class membership of the input image by using the softmax activation function to transform the model's raw outputs into probability distributions across classes.

Table 2 graphical representation of the EfficientNetB3 model architecture.

Table 2. Architecture of proposed EfficientnetB3 model

Parameter	Value
Input Image Dimensions	A 224x224 pixel image using RGB color channels
Base Pre-trained Model	EfficientNetB3 for feature extraction with fully linked layers omitted (include top=False)
Batch Normalization	Increases training speed and stability by adjusting layer outputs
Dense Layer 1	Includes L2 weight regularization, L1 activity regularization, and L1 bias regularization; dense layer with 256 neurons and ReLU activation
Dense Layer 1	Dropout layer with a rate of 0.45 to prevent overfitting
Dense Layer 2 (Output)	Neurons in the final dense layer that correspond to class count and softmax activation

Table 3 displays the model's values and parameters during the training process, and Figure 3 displays a graphic representation of the suggested model's architecture.

Table 3. Parameters of the proposed model and values during the training process

Parameter	Value
Epocs	10
Verbose	1
Validation steps	None
Shuffle	Flase

Results and Discussion

Following the model's development, we evaluated EfficientNte-B3's performance. We also discover the performance of the simpleCNN model. We calculate accuracy, recall, F-score, and precision. We will also show the suggested model's training, validation, loss, and accuracy curves. The confusion matrix for our EfficientnetB3 model was finally calculated. We assessed the performance of two distinct DL models in the context of our study, namely, the SimpleCNN and the EfficientNetB3 model— which centred on the early identification of lung cancer. A wide range of evaluation standards, such as precision, recall, F-score, and accuracy, were used to evaluate the models thoroughly. Notably, the findings revealed a significant variation in how well different models performed.

The SimpleCNN model performed admirably, with precision, recall, F-score, and accuracy values of 83%, 86%, 84.5%, and 85%, respectively. Comparatively, the EfficientNetB3 model demonstrated remarkable results across all measures, having 100% accuracy, 100% precision, and 100% recall. The implications of these findings on the performance of lung cancer diagnosis are important. In closing, our research led to a comparison analysis that overwhelmingly preferred the EfficientNetB3 model, and its unmatched accuracy, recall, precision, and F-score highlight its strength and competence in detecting lung cancer cases. The EfficientNetB3 model outperformed the SimpleCNN model, which also performed admirably, but its success highlights how it has the potential to dramatically enhance the precision and dependability of lung cancer detection systems.

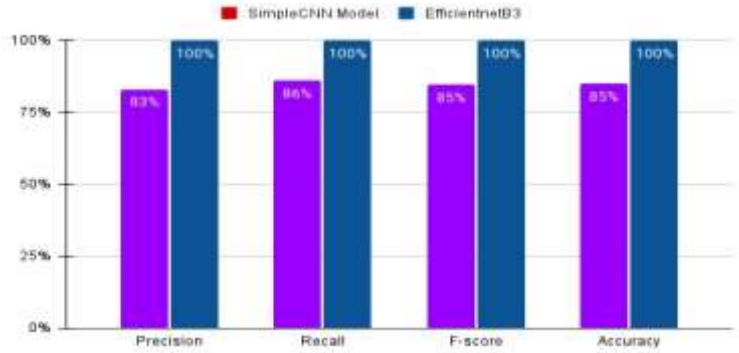

Figure 4. The evaluation metrics of our proposed model

Two distinct classifiers, SimpleCNN and EfficientNetB3 Model, and their performance metrics are displayed in Table 4.

Table 4. Parameters of the proposed model and values

Classifier	Precision	Recall	F-score	Accuracy
SimpleCNN Model	83%	86%	84.5%	85%
EfficientnetB3	100%	100%	100%	100%

Monitoring the training and validation metrics is essential for determining a model's effectiveness and generalizability in DL, especially for applications like lung cancer diagnosis. Training and validation loss and training and validation accuracy are two crucial measures that are crucial for assessing model performance. Loss is a key indicator that measures how well a model's forecasts correspond to the actual labels in the ground truth data. The training loss in the context of lung cancer detection refers to how well the model fits the training set of data. In contrast, validation loss assesses how

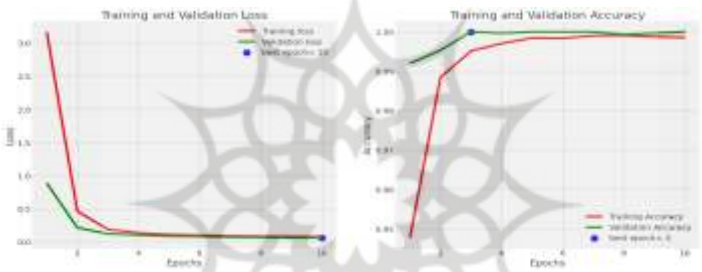

Figure 5. Training and validation loss of the proposed model

The model performs on untested data, replicating its adaptability to novel, untested situations. Overfitting can be discovered by observing the training and validation loss. The model fits the training data too closely and may not generalize well if the training loss keeps dropping while the validation loss rises. Loss function minimization is the aim of model training. To improve the model's performance, changes can be made to its architecture, hyperparameters, or regularization methods by evaluating the training and validation loss. Figure 5 shows the training and validation loss and training and validation accuracy of our proposed EfficientnetB3 model. Another important indicator is accuracy, which shows the percentage of correctly identified occurrences relative to all instances. While validation accuracy demonstrates how effectively the model generalizes to fresh, untested data, training accuracy demonstrates how well the model performs on the training data. The training and validation accuracy over time can be tracked to determine how well the model improves. Overfitting may be indicated by rapidly increasing training accuracy but stagnant or declining validation accuracy. The graphs in Figure 5 show the trends in training and validation accuracy throughout 10 epochs, as well as training and validation loss.

The epoch number (x-axis) and the corresponding metric values (y-axis) are displayed on both curves. These curves' convergence throughout the 10 epochs indicates that the model is stabilizing and achieving a level of performance that is largely consistent. The confusion matrix of the proposed model is shown in Figure 6. In the field of medical diagnostics, such as the diagnosis of lung cancer, evaluating an ML model's performance extends beyond only considering accuracy and loss. A confusion matrix offers a more thorough understanding of how well a model categorizes various kinds of cases. Four categories are used to categorize the predictions and actual labels: true positives, true negatives, false positives, and false negatives. Particularly in the context of lung cancer diagnosis, a confusion matrix offers a more comprehensive evaluation of a model's performance than accuracy alone.

Discussion and Comparison with Existing Work in Deep Learning:

Table 5. Comparison of lung cancer classification outcomes of existing methods and histopathological images datasets

Model	Accuracy
Deep Neural Network (DNN)	95%
Convolutional Neural Network (CNN)	97.89%
CNN	97.2%
EfficientNetB3	100%

In Table 5, we compare our proposed model with the existing one using the DL model and histopathological images dataset.

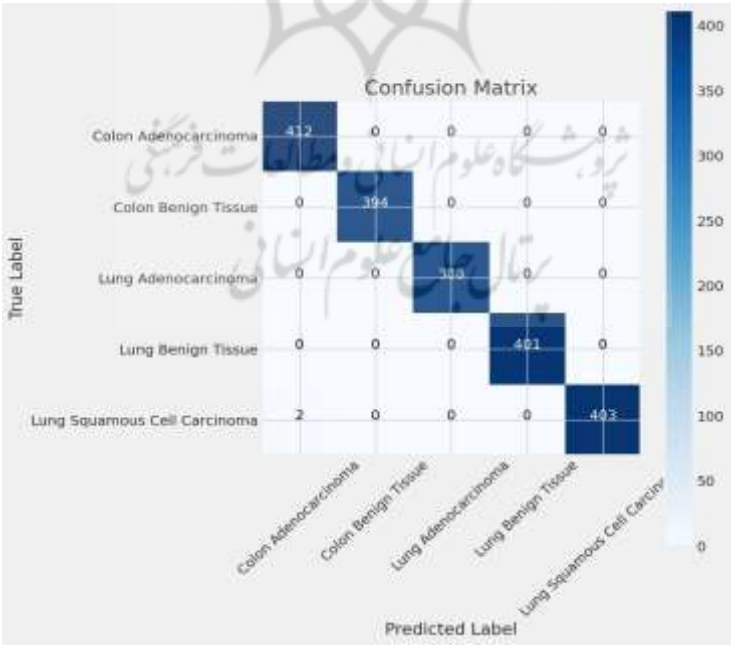

Figure 6. Confusion matrix

Recently, DNN and Machine Learning have made considerable strides, especially in the area of image classification. An admirable accuracy of 95% was attained by a DNN in (Mohalder, 2022), while an even higher accuracy of 97.89% was achieved by a CNN. Another study (Mangal, 2020) also used CNN which produced outcomes with a 97.2% accuracy. These findings showed how image classification methods are continually improving.

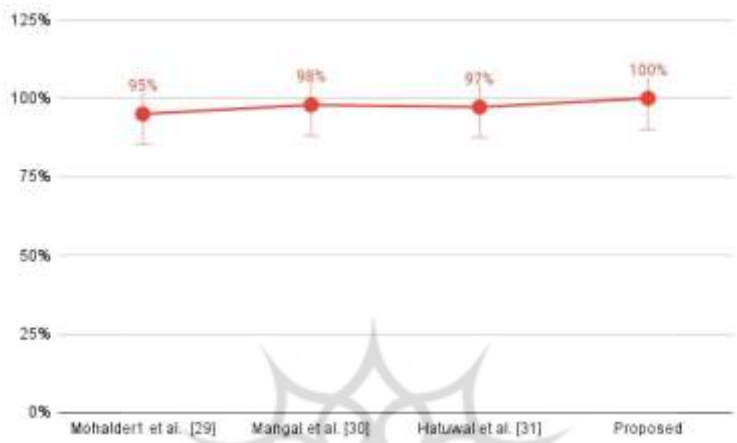

Figure 7. Comparison of lung cancer classification results of existing methods with our proposed model

However, we presented a revolutionary approach that acquired an unmatched accuracy of 100% by employing the EfficientNetB3 architecture. In addition, our suggested model performs better than existing methods in terms of accuracy to enhance efficiency and effectiveness in image classification tasks. Our EfficientNetB3 model reached an exquisite accuracy of 100% that surpassed (21) and (28), which attained accuracies of 95% and 97.2%, also outperforming the previous best of 97.89% from (5) and demonstrating significant progress in image categorization. Our model represented a significant advancement in the field of image classification and holds tremendous potential for many real-world applications due to the overall advantages of improved accuracy and efficiency. Figure 7 illustrates the classification outcomes that compare existing work with our proposed model.

Conclusion

Colon and lung cancer are major contributors to global mortality. Lung cancer detection has made significant progress through advanced technology and methods. While SimpleCNN and EfficientNetB3 models have been highly accurate, they face challenges in interpretability and generalizability into current medical procedures. Our study presented the effectiveness of deep learning-based classifier models, specifically the EfficientNetB3 architecture, in detecting and classifying lung cancer utilizing histopathological image data. It outperformed SimpleCNN in multiple evaluation metrics, with exceptional accuracy, recall, F1 score, and

overall performance. Future research will enhance pulmonary nodule categorization, refine the model, and address interpretability and practical integration challenges. The dataset will be expanded, and healthcare professionals will collaborate to ensure the successful translation of these advancements into clinical practice; this will enhance the quality of care for people at risk of lung cancer, ultimately enhancing survival rates.

Conflict of interest

The authors declare no potential conflict of interest regarding the publication of this work. In addition, the ethical issues including plagiarism, informed consent, misconduct, data fabrication and, or falsification, double publication and, or submission, and redundancy have been completely witnessed by the authors.

Funding

The author(s) received no financial support for the research, authorship, and/or publication of this article.

References

Ahmed, S. T. (2022). 6G enabled federated learning for secure IoMT resource recommendation and propagation analysis. *Computers and Electrical Engineering*, 108210.

Alakwaa, W. a. (2017). Lung cancer detection and classification with 3D convolutional neural network (3D-CNN). *International Journal of Advanced Computer Science and Applications*.

AlZubaidi, A. K. (2017). Computer aided diagnosis in digital pathology application: Review and perspective approach in lung cancer classification. *2017 annual conference on new trends in information \& Communications technology applications (NTICT)* (pp. 219--224). IEEE.

Bhaktavastalam, P. a. (2016). Lung cancer disease analyzes using pso based fuzzy logic system. *Int J Res Eng Technol*, 69--71.

Bhattacharjee, A. a. (2022). A hybrid approach for lung cancer diagnosis using optimized random forest classification and K-means visualization algorithm. *Health and Technology*, 787--800.

Bhuvaneswari, P. a. (2015). Detection of cancer in lung with k-nn classification using genetic algorithm. *Procedia Materials Science*, 433--440.

Bonavita, I. a.-P. (2020). Integration of convolutional neural networks for pulmonary nodule malignancy assessment in a lung cancer classification pipeline. *Computer methods and programs in biomedicine*, 105172.

Borkowski, A. A. (2019). Lung and colon cancer histopathological image dataset.

Borkowski, A. A. (2019). Lung and colon cancer histopathological image dataset (lc25000). *arXiv preprint arXiv:1912.12142*.

de la Rosa, J. J.-P.-S.-M. (2013). Higher-order statistics: Discussion and interpretation. *Measurement*, 2816--2827.

Dimililer, K. a. (2017). Tumor detection on CT lung images using image enhancement. *The Online Journal of Science and Technology*, 133--138.

Dritsas, E. a. (2022). Lung cancer risk prediction with machine learning models. *Big Data and Cognitive Computing*, 139.

Hatuwal, B. K. (2020). Lung cancer detection using convolutional neural network on histopathological images. *Int. J. Comput. Trends Technol*, 21--24.

Hatuwal, B. K. (2020). Lung cancer detection using convolutional neural network on histopathological images. *Int. J. Comput. Trends Technol*, {21--24.

Kalaivani, N. a. (2020). Deep learning based lung cancer detection and classification. *IOP conference series: materials science and engineering* (p. {012026). IOP Publishing.

Krishnaiah, V. a. (2013). Diagnosis of lung cancer prediction system using data mining classification techniques. *International Journal of Computer Science and Information Technologies*, 39--45.

Kumar, A. a. (2023). Augmented Intelligence enabled Deep Neural Networking (AuDNN) framework for skin cancer classification and prediction using multi-dimensional datasets on industrial IoT standards. *Microprocessors and Microsystems*, 104755.

Lakshmanaprabu, S. a. (2019). Optimal deep learning model for classification of lung cancer on CT images. *Future Generation Computer Systems*, 374--382.

Liu, S. a. (2017). Pulmonary nodule classification in lung cancer screening with three-dimensional convolutional neural networks. *Journal of Medical Imaging*, 041308--041308.

Makaju, S. a. (2018). Lung cancer detection using CT scan images. *Procedia Computer Science*, 107--114.

Mangal, S. a. (2020). Convolution neural networks for diagnosing colon and lung cancer histopathological images. *arXiv preprint arXiv:2009.03878*.

Manju, B. a. (2021). Efficient multi-level lung cancer prediction model using support vector machine classifier. *IOP Conference Series: Materials Science and Engineering* (p. 012034). IOP Publishing.

Mohalder, R. D. (2022). Lung Cancer Detection from Histopathological Images Using Deep Learning. *International Conference on Machine Intelligence and Emerging Technologies* (pp. 201--212). Springer.

Nasrullah, N. a. (2019). Automated lung nodule detection and classification using deep learning combined with multiple strategies. *Sensors*, 3722.

Prisciandaro, E. a. (2023). Artificial Neural Networks in Lung Cancer Research: A Narrative Review. *Journal of Clinical Medicine*, 880.

Rong, Z. a. (2021). Diagnostic classification of lung cancer using deep transfer learning technology and multi-omics data. *Chinese Journal of Electronics*, 843--852.

Roy, S. a. (2021). Comparative Study of Machine Learning Algorithms for Detecting Breast Cancer. *International Journal of Computer Science Trends and Technology (IJCST)*, 103--111.

Sang, J. a. (2019). Automated detection and classification for early stage lung cancer on CT images using deep learning. *Pattern recognition and tracking XXX* (pp. 200--207). SPIE.

Shandilya, S. a. (2022). Analysis of lung cancer by using deep neural network. *Innovation in Electrical Power Engineering, Communication, and Computing Technology: Proceedings of Second IEPCCT 2021* (pp. 427--436). Springer.

Singh, G. A. (2019). Performance analysis of various machine learning-based approaches for detection and classification of lung cancer in humans. *Neural Computing and Applications*, 6863--6877.

Sun, W. a. (2016). Computer aided lung cancer diagnosis with deep learning algorithms. *Medical imaging 2016: computer-aided diagnosis* (pp. 241--248). SPIE.

Tan, M. a. (2019). Efficientnet: Rethinking model scaling for convolutional neural networks. *PMLR*, (pp. 6105--6114).

Viale, P. H. (2020). The American Cancer Society's facts \& figures: 2020 edition. *Journal of the Advanced Practitioner in Oncology*, 135.

Wang, X. a.-A. (2022). Weakly supervised learning for whole slide lung cancer image classification. *Medical imaging with deep learning.*

Bibliographic information of this paper for citing:

Sudhakar, Bolleddu; Sikrant, Poornima A; Prasad, M Lakshmi; Latha, S Bhargavi; Kumar, G Ravi; Sarika, Sabavath & Shaker Reddy, Pundru Chandra (2024). Efficient NetB3 for Enhanced Lung Cancer Detection: Histopathological Image Study. *Journal of Information Technology Management,* 16 (1), 98-117. https://doi.org/ 10.22059/jitm.2024.96377